LASER INTERFEROMETER GRAVITATIONAL WAVE OBSERVATORY
-LIGO-
CALIFORNIA INSTITUTE OF TECHNOLOGY
MASSACHUSETTS INSTITUTE OF TECHNOLOGY

Technical Note **LIGO-T080334-00-Z** 2008/12/08

S5 First-Year High-Frequency Burst Search Review Report

Ik Siong Heng[1] (chair), Jonah Kanner[2], Matthew Pitkin[1]
(S5 First-Year High-Freq review sub-committee)
Brennan Hughey[3], Michele Zanolin[4]
[1]University of Glasgow
[2]University of Maryland
[3]LIGO - Massachusetts Institute of Technology
[4]Embry-Riddle Aeronautical University

DRAFT: Circulation restricted to members of the LIGO Scientific Collaboration.

This is an internal working note
of the LIGO Project

California Institute of Technology
LIGO Project - MS 51-33
Phone (626) 395-2129
Fax (626) 304-9834
E-mail: info@ligo.caltech.edu

Massachusetts Institute of Technology
LIGO Project - MS 20B-145
Phone (617) 253-4824
Fax (617) 253-7014
E-mail: info@ligo.mit.edu

http://www.ligo.caltech.edu

File printed: 2008/12/08

Abstract

This document is the report by the S5 First-Year High-Frequency review sub-committee on the paper, *Search for High Frequency GravitationalWave Bursts in the First Calendar Year of LIGO's Fifth Science Run* (LIGO-P080080-00-Z) and the analysis presented therein. The paper and the analysis have been examined carefully by the review team and the principal authors. We believe the results of the paper to be correct, interesting and well-presented. We recommend that the LSC Executive Committee approve the paper for publication.

Contents

I. OVERVIEW OF THE S5 FIRST-YEAR HIGH-FREQUENCY BURST SEARCH AND PAPER

The S5 first-year high-frequency burst paper reports on a search for burst gravitational waves in a frequency band spanning 1 to 6 kHz. No gravitational wave candidates were observed and upper limits are set. The larger calibration uncertainties led to the decision not to use the null-stream and R0 cuts. Moreover, the shot-noise dominated noise at these frequencies is significantly more stationary than at lower frequencies, so the impact of these cuts at higher frequencies is reduced. A detection-only search for gravitational waves in H1H2-only livetime is also performed. Again, no gravitational wave candidates were observed.

In the sections below, relevant portions of the text from the paper is highlighted and important details discussed. A link to the paper draft can be found at [1].

A. Abstract

We present an all-sky search for gravitational waves in the frequency range 1 to 6 kHz during the first calendar year of LIGO's fifth science run. This is the first untriggered LIGO burst analysis to be conducted above 2 kHz. We discuss the unique properties of interferometric data in this regime. No gravitational events above threshold were observed, but upper limits on gravitational wave emission in this frequency range are presented. Implications for specific theoretical models of gravitational wave emission are also discussed.

The reviewers think the abstract is concise and accurate.

B. Introduction

The LIGO detectors are introduced here and the S5 run is described to the reader. It highlights the fact that this is the first search for gravitational waves performed at frequencies higher than 2 kHz and discusses the rationale behind this.

C. Transient sources of few-kHz gravitational waves

In this section, possible sources of gravitional waves in the frequency band analysed are discussed. The sources listed and discussed are:

- core-collapse supernova
- the formation of a rotating black hole due to neutron star collapse
- a hypermassive neutron star resulting from the merger of two neutron stars
- gravitational wave emission at the neutron star normal modes
- an accreting neutron star undergoing torque-free precession
- low mass black hole mergers
- preon star mergers
- cosmic string cusps

A generic burst search (as opposed to matched filtering) is performed for signals from these sources because the models used to generate waveforms from these models have significant uncertainties.

D. Data analysis

The search pipeline is described in this section. This search uses Q-pipeline to generate single-detector triggers before using CorrPower to test the consistency of the waveforms of the detected signal between the three interferometers. The descriptions are quite standard (condensed from the references) and many aspects of the analysis (cuts and tuning) are similar to what has been done in previous analyses. There are a few notable differences.

For the Q-pipeline, a threshold of normalised energy Z=16 was chosen. This is a relatively low waveform with a view that CorrPower will reject the majority of the triggers as glitches. So, the CorrPower Γ threshold will have the greatest effect on the sensitivity. Additionally, the analysis blocks were reduced from 64 tp 16 seconds due to memory constraints and the templates stop at a maximum of Q=32.

The data quality cuts and vetoes were applied next. This search uses the same category 1 and 2 flags as those used by the low frequency search. The category 3 flags applied here are a subset of those employed by the low frequency search. This is because many of the standard category 3 flags were observed to remove times which did not show a statistically significant excess in the high frequency trigger rate. Additionally, a few of the category 3 flags were observed to veto a statistically significant portion of the hardware injections. This search also does not employ the Q-pipeline null stream test. The null stream test did not veto a significant portion of triggers while increased calibration uncertainty meant that there was a non-negligible and difficult to measure probability of vetoing any actual gravitational wave signals present in the data.

In the higher frequency regime, CorrPower requires additional notch filters to damp mechanical resonances that can generate spuriously large Γ values. Notch filters with Q=400 were applied at frequencies of 3727.0, 3733.7, 5470.0 and 5479.2 Hz before the data was whitened. The R0:H1H2 cut was not applied here because it was observed that hardware injections have a negative R0:H1H2 value at high frequencies. Background studies led to the choise of a Γ threshold of 6.2. This yields a false alarm rate of of $10^{-8}\,Hz$.

E. Properties of LIGO data above 1 kHz

The high frequency trigger distribution and the calibration uncertainty are presented in this section. A comparison of the trigger distribution shows a much longer tail in the lower frequency ($< 1\,kHz$) trigger distribution than for the higher frequency triggers. This is attributed the stationarity of noise in this shot-noise dominated regime.

The calibration uncertainties are stated to be $\sim 8\%$ at $1\,kHz$ and $\sim 45\%$ at $6\,kHz$ in amplitude with an addition 2 to 6% from the h(t) conversion. A phase uncertainty of 70° close to $5.5\,kHz$ is also stated. As of these uncertainty values have not been approved by the calibration review committee.

The use of the long wavelength approximation in determing the antenna patterns at these higher frequencies is also discussed. It has been demonstrated by applying the fully correct antenna pattern at 6 kHz and comparing to the results of the long wavelength approximation that this approximation is still valid in this regime and that the errors introduced are on the order of 1-2% and therefore dwarfed by other errors and uncertainties.

F. Detection efficiency

The detection efficiency, characterised by $h_{\rm rss}^{50\%}$, is evaluted in this section. Using the BurstMDC and GravEn packages, sine-Gaussian (1053 to 5000 Hz) and Gaussian (0.05 to 0.25 ms) signals were injected. In addition to these signals, the D1 and D4 waveforms from Baiotti and Rezzola were also injected. The $h_{\rm rss}^{50\%}$ has been obtained for all injected signals and a graph of efficiency versus distance plotted for for the D1 and D4 waveforms.

The detection efficiency for hardware injections is also discussed in this section. All injections with $h_{\rm rss} > 7\times10^{-21}$ were recovered. One should note that there is no antenna pattern included in the calculation of $h_{\rm rss}$ values for the hardware injections.

G. Results

The statistics of the time-shifted triggers and the zero-lag observations are reported here. No zero-lag triggers were found above Γ threshold of 6.2. For low thresholds ($\Gamma > 2$), 193 triggers were observed when 172.1 were expected. The probability of having this excess is 6.2% and is, therefore, not a significant deviation from the expected trigger count. A follow-up of the loudest Γ zero-lag triggers is performed by studying the Q-scans of these triggers. None of these triggers appeared significant and, in all cases, only 1 of the 3 interferometers had any substantial excess power. The upper limit on the rate of burst gravitational waves in the frequency band of this search is set for the H1H2L1 livetime.

A "detection-only" search is performed on H1H2-only data and reported in this section. No zero-lag triggers were found above the thresholds set by studies on time-shifted coincidence triggers.

H. Summary and future directions

The search is summarized in this section and the observation that no gravitational wave candidates is clearly stated. The prospects of improvements to the LIGO and Virgo detectors are discussed with a view to the possibility of performing this search on the better quality data available in the future.

II. REVIEW

A. Scope of the review

This analysis is a search for gravitational waves using Q-pipeline. No candidates are found above the threshold and an upper limit is set. Since the Q-pipeline code has been reviewed by a different team, the review concentrated on supporting framework used to produce the presented results. The review team also check tests performed to demonstrate the robustness of the search to large calibration uncertainties. While this robustness was demonstrated, as of December 8, 2008, the calibration review committee has not approved the values stated for calibration uncertainty in the paper.

In addition to the analysis scripts, DQ flags and results, the review team also checked the data conditioning of the high-frequency core-collapse waveforms used to characterise the sensitivity of the search. The H1H2-only search is also reviewed because a paragraph in the paper states that a search for gravitational waves was performed in this data and no candidates were found. For a link to the reviewed items described below, see [2]. The paper draft can be found at [1].

B. Q-pipeline parameter files

The Q-pipeline input parameters were checked. Many of the parameter values were found to be identical to those used in the low frequency search, or modified in an obvious way for the high frequency search (i.e. the frequency range and Q range were changed as expected).

The block time was reduced from 64 seconds to 32 seconds. This block time was found to be consistent with the block time required to train the whitening filter (i.e. the training time is much greater than the time of expected signal length), and so this not a problem.

There was some discussion about the presence of parameters for the null stream veto. However, the veto is, in fact, turned off, so parameters modifing the null stream veto are vestigial.

The *extraBlockOverlap* parameter was chosen to be 1, as compared with 0 in the low-frequency search. This parameter leads to an extra second of data included in the filter training, i.e. 1 second of overlapped data that is used to train both filters on adjacent blocks. There is no reason to believe this negatively impacts the search.

Another parameter, *CorrelationFactor*, was set to 0.1 for the high frequency search, compared with 0 for the low frequency search. This parameter effects the condition used to cut triggers in the H1H2 analysis. Brennan re-ran the H1H2 analysis with this parameter turned to zero. He discovered that the triggers cut based on this parameter were all low-energy. In fact, in the entire first year analysis, none of the triggers passing the eventual H1H2 threshold were affected by this parameter (i.e. the results of the analysis were identical whether this parameter was set to 0 or 0.1).

The review committee concludes that the parameters used for the Q-Pipeline portion of the analysis are appropriate.

C. Analysis and post-processing scripts

All scripts used by the analysis were checked [3]. The scripts used to produce dag files and file caches were duplicated and observed to produce identical outputs to those used in the analysis. Such tests were also performed on scripts used to apply data quality vetoes. Scripts were also inspected and found to be sensible.

Some discrepancies were observed, but these were inconsequential and were just the result of slightly different versions of the scripts being posted on the review page than those used in the actual analysis. These issues were resolved and the final scripts used in the analysis were inspected and found to produce sensible and consistent results.

D. Data quality flags

To check that the data quality flags were applied properly, the data quality scripts were inspected and rerun. There was a minor discrepancy found in the segment lists after apply cat 1 data quality flags. This was because the longest segment was split into two shorter segments to avoid having a large chunk of analysis processed by a single node in the cluster, thereby speeding up the data processing. There were no problems found with the segments after the application of cat 2 and cat 3 data quality flags. A page reporting on these checks can be found at [4].

E. Zero-lag and background results

The trigger statistics and threshold choices were discussed with the review sub-committee before the zero-lag results were generated. The distribution of the background and the shape of the efficiency curves looked reasonable. The $h_{rss}^{50\%}$ points were about a factor of 10 greater than the noise amplitude density at each frequency which is consistent with what has been observed in previous analyses. The whitening performed by CorrPower was also checked. The notch filteres were observed to be supressing the known resonances in the data well and there were no anomalies in the whitened data.

The R0:H1H2 cut in CorrPower was not used because injections about 3 kHz were producing negative R0:H1H2. The null-stream cut is also not applied because of worries that the larger calibration uncertainty at these frequencies will lead to a significant fraction of signals being vetoed. Since the noise is more stationary at these higher frequencies, not much should be gained when apply these cuts anyway, so the review sub-committee is fine with this.

A bug was found in the use of CorrPower which meant that some data were being low-pass filtered multiple times instead of just oncei [5]. The analysis was rerun after this bug was fixed and very little change in the statistics of the background and zero-lag triggers were observed. There were still no zero-lag triggers above the chosen $\Gamma > 6.2$ threhold. The efficiencies were also virtually unchanged (within $i \sim 1\%$). The review sub-committee felt that the bug fix and supporting documentation was satisfactory. The figures in the paper reflect the new (correct) results.

F. H1H2-only analysis

The H1H2-only pipeline and the time-shifted results it produced were presented to the review sub-committee [6]. The choice of cuts and the scripts used were found to be sensible and the review sub-committee approved the pipeline. The zero-lag results were then generated and no triggers above the chosen threshold of $\Gamma > 10$ was observed. The loudest zero-lag trigger had a Γ value of 8. All the scripts used to produce the H1H2 results were inspected and found to be sensible.

G. Astrophysically-motivated waveforms

The script applied to the core-collapse waveforms generated by Baiotti and Rezzolla was reviewed [7]. The script filters and resamples the waveforms as well as converting the amplitude of the waveforms into strain. The conversion factor used in the script was checked and rederived. The script was checked and rerun to produce the expected waveform. The waveform plotted in the later versions of the paper were found not to match the output of the reviewed script. The plotted waveforms were found to be wrong and the correct waveforms were plotted in subsequent versions.

H. Plot scripts

The plot scripts for all figures (except Figure 2, which was produced by hand) were checked [3] and found to reproduce the figures in the paper.

III. FOLLOWING UP LOUDEST TRIGGERS BELOW THRESHOLD

Q-scans were run on the two loudest Γ zero-lag triggers below threshold. These two triggers had Γ values that were about 5.5. There was no particular feature that stood out about these triggers. Additionally, there were no

GCN alerts posted around the time of these triggers.

A. GPS second 820482568

This occurred on Jan 5 2006 at 7:49:14 UTC. The central frequency of the trigger is 1800 Hz with a Γ of 5.5. It occurred more than 1000 seconds away from the nearest acquisition and loss of lock by any of the 3 detectors. Only the Science flags were "on" at the time of this trigger.

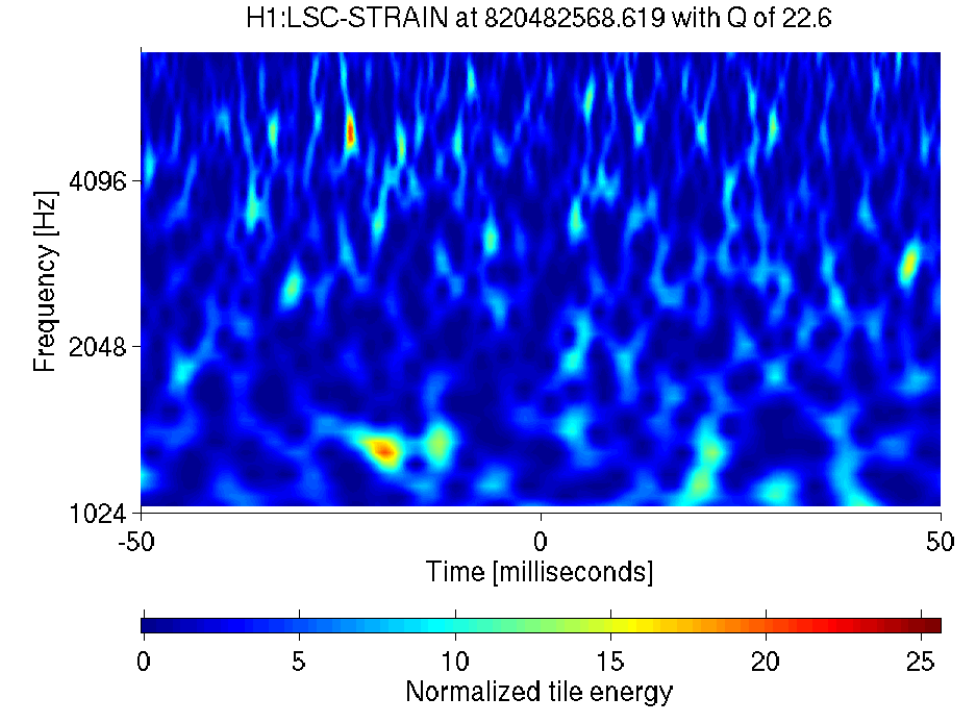

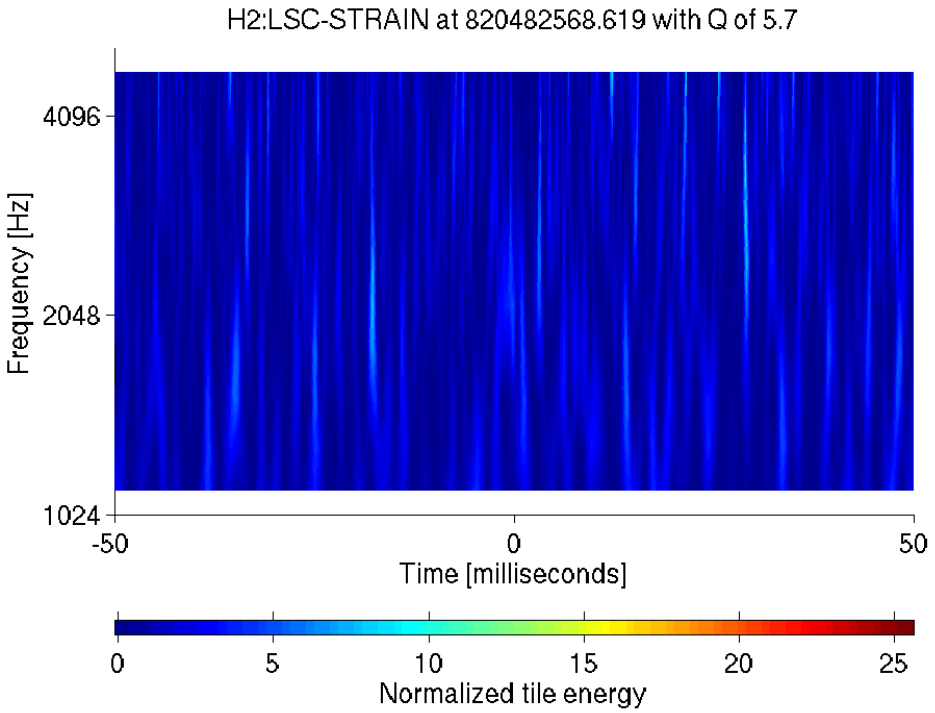

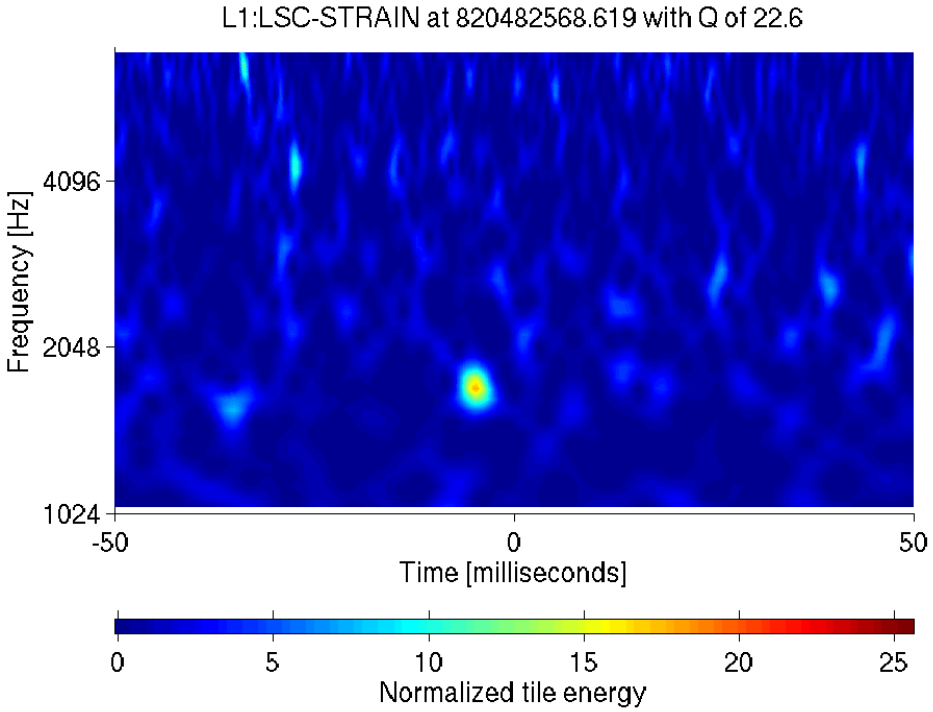

B. GPS second 840633446

This trigger occurred on Aug 26 2006 at 13:17:12 UTC. The central frequency of the trigger is 4300 Hz, with a Γ of 5.3. This trigger was also observed more than 100 seconds away from an lock loss (acquisition), The data was flag by several data quality flags though they are mainly pulsar injection flags. In L1, however, the ELEVATED GLITCHINESS flag was in force and it was not long before a series of overflow flags were triggered.

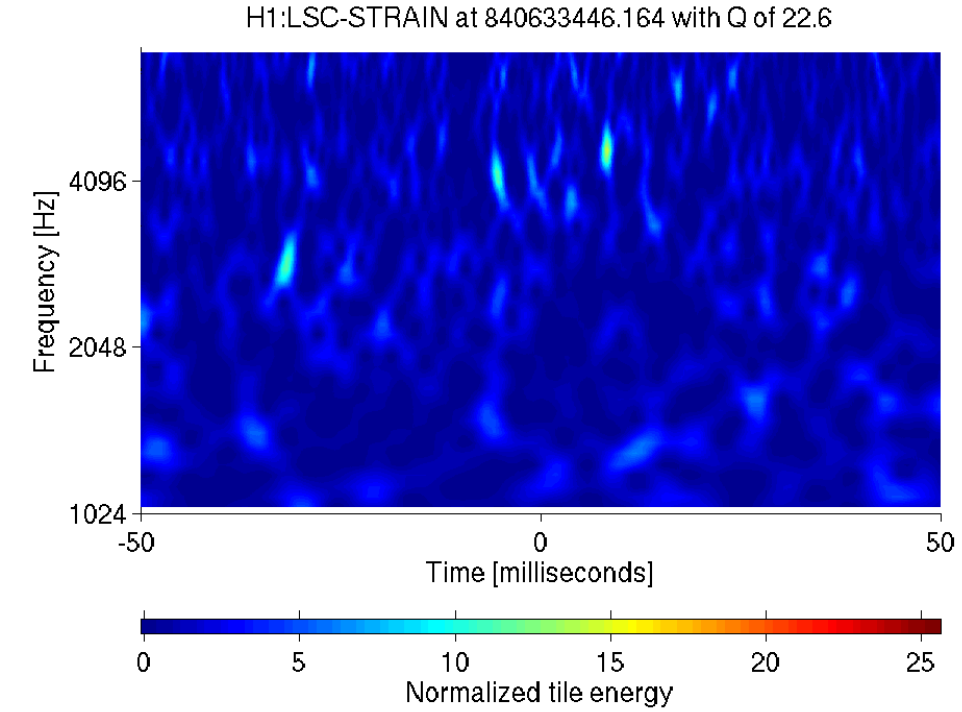
H1:LSC-STRAIN at 840633446.164 with Q of 22.6
Frequency [Hz]
4096
2048
1024
-50
0
50
Time [milliseconds]
0
5
10
15
20
25
Normalized tile energy

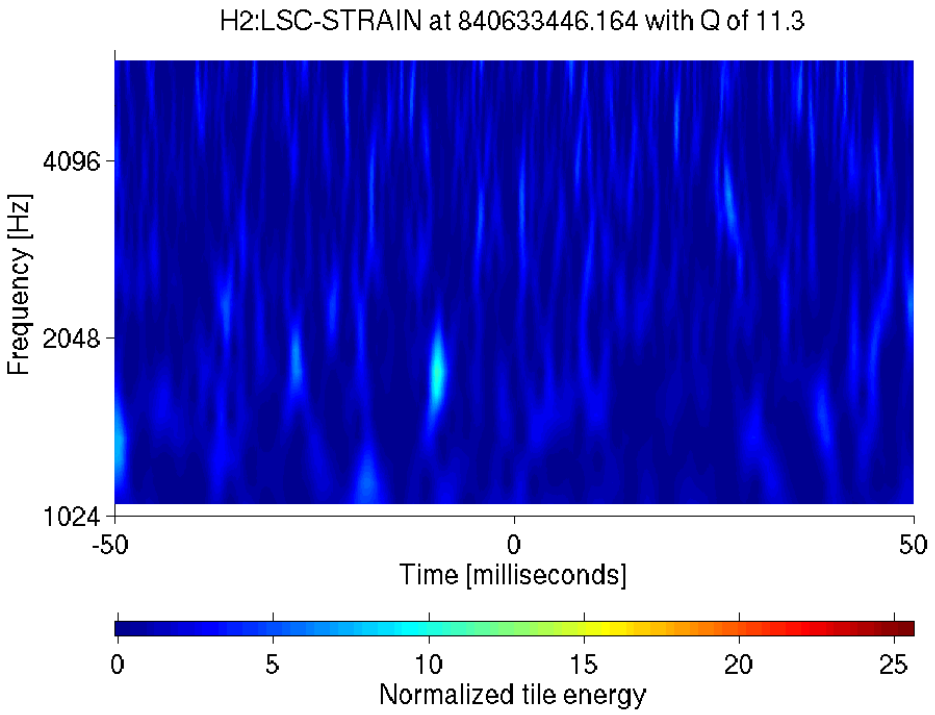
H2:LSC-STRAIN at 840633446.164 with Q of 11.3
Frequency [Hz]
4096
2048
1024
-50
0
50
Time [milliseconds]
0
5
10
15
20
25
Normalized tile energy

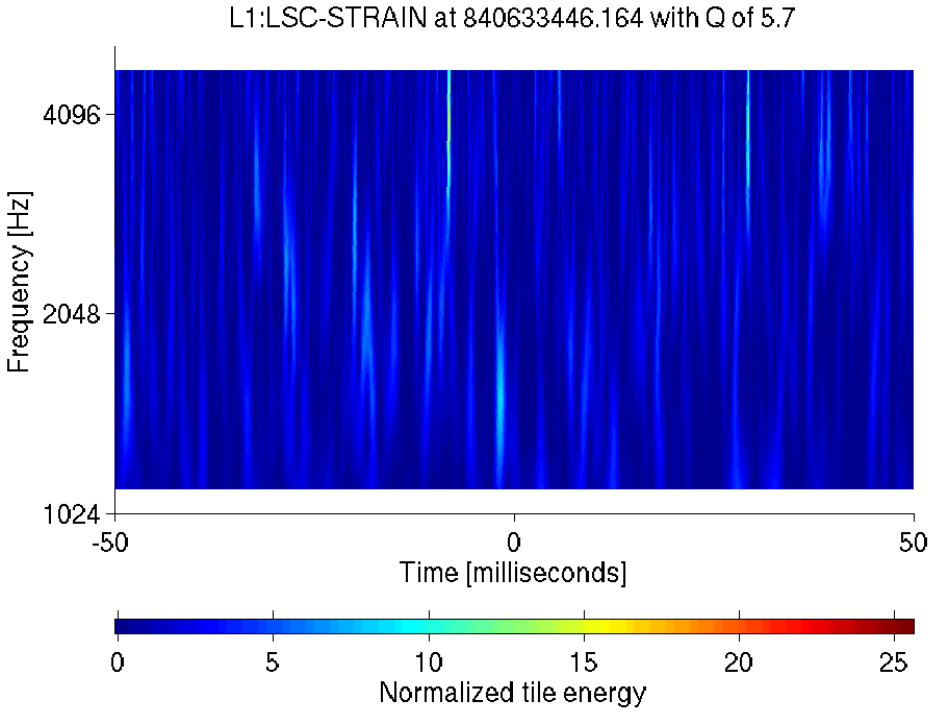

IV. SENSITIVITY ESTIMATE

In this section we describe the statistical nature of the LIGO noise and how we model the calculations of the Corrpower Γ. A link to the original workings and documentation for this can be found at [8]. In the first part we describe the statistical properties of the Corrpower Γ for an arbitray, but stationary around the event, power spectral density. In the second part we adapt the analysis to the sensitivity estimate performed in the HFS where Corr Power is passed whitened data (and the signal is whitened too).

Let us consider the calibrated noise at the 3 detectors $h_1(t)$, $h_2(t)$ and $l_1(t)$.

Assumption 1: the 3 noise time series are uncorrelated, stationary stochastic processes charaterized by their mean and autocorrelation functions:

$$< h_1(t) >=< h_2(t) >=< l_1(t) >= 0 \tag{1}$$

$$< h_1(t)h_2(t) >=< h_1(t) >< h_2(t) >= 0 \tag{2}$$

$$< h_1(t)l_1(t) >=< h_1(t) >< l_1(t) >= 0 \tag{3}$$

$$< h_2(t)l_1(t) >=< h_2(t) >< l_1(t) >= 0 \tag{4}$$

$$< h_1(t)h_1(t+\tau) >= R_1(\tau) \tag{5}$$

$$< h_2(t)h_2(t+\tau) >= R_2(\tau) \tag{6}$$

$$< l_1(t)l_1(t+\tau) >= R_3(\tau) \tag{7}$$

It can be proven, see Willsky-6432-MIT-EE-textbook-1999, that the relationships between the autocorrelation functions and the noise power spectral density at each interferometer are given by

$$R_1(\tau) = \int_{-\infty}^{\infty} e^{-i2\pi ft} S_{H1}(f) df \tag{8}$$

$$R_2(\tau) = \int_{-\infty}^{\infty} e^{-i2\pi ft} S_{H2}(f) df \tag{9}$$

$$R_3(\tau) = \int_{-\infty}^{\infty} e^{-i2\pi ft} S_{L1}(f) df \tag{10}$$

where $S_{H1}(f)$, $S_{H2}(f)$ and $S_{L1}(f)$ are the available noise power spectral densitities. CorrPower computes the r-statistic over 3 different coincidence windows, T_1, T_2 and T_3 and for each of them evaluates:

$$r_t = \frac{\int_{-T/2}^{T/2} x_\alpha(t) x_\beta(t+\tau) dt}{||x_\alpha(t)||||x_\beta(t+\tau)||} \tag{11}$$

where α,β=1,2,3 are indices running through different interferometer and

$$N_\alpha = ||x_\alpha(t)|| = \sqrt{\int_{-T/2}^{T/2} x_\alpha(t)^2 dt} \tag{12}$$

I assume that the energy in the noise does not depend on the exact location of the temporal window and that it is simply proportional to the duration of the window.This is a consequence of the assumption of noise stationarity and of having integration windows of time much longer than the periods of interest. The value of N_α fluctuates less and less for longer windows becoming a constant and not a random variable. We therefore assume that N_α can be expressed as:

$$N_\alpha = T n_\alpha, N_\beta = T n_\beta \tag{13}$$

where n_α and n_β are not random variables. A first ingredient to evaluate the probability distribution of the Γ evaluted by CorrPower is to evaluate the PDF of the r statistics. However since we treat the denominator as a constant we need to estimate the probability distribution of the numerator:

$$\hat{r}_T = \int_{-T/2}^{T/2} x_\alpha(t) x_\beta(t+\tau) dt = \sum_{i=1}^{N} x_\alpha(t_i) x_\beta(t_i+\tau) \Delta t \tag{14}$$

where the right hand side describes the discretization in place when the a practical calculation is performed. Another assumption: N is large enough that the central limit throerem applies to 14, so $\hat{r}_T$ becomes gaussian with mean and variances given by

$$< \hat{r}_T >= \sum_{i=1}^{N} < x_\alpha(t_i) >< x_\beta(t_i+\tau) > \Delta t = 0 \tag{15}$$

$$\begin{aligned}
\sigma^2_{T_1} =< \hat{r}^2_T > &= \sum_{i=1}^{N}\sum_{j=1}^{N} < x_\alpha(t_i) x_\beta(t_i+\tau) x_\alpha(t_j) x_\beta(t_j+\tau) > \\
&= \sum_{i=1}^{N}\sum_{j=1}^{N} < x_\alpha(t_i) x_\alpha(t_j) >< x_\beta(t_i+\tau) x_\beta(t_j+\tau) > \\
&= \sum_{i=1}^{N}\sum_{j=1}^{N} R_\alpha(t_i - t_j) R_\beta(t_i - t_j)
\end{aligned}$$

Not including, for now, the effect of the maximization over τ, the probability of r_{T_1} becomes

$$p(r_{T_1}) = \frac{1}{\sqrt{2\pi(\sigma^2_{T_1}/(N^2_\alpha N^2_\beta)}} exp(-\frac{r_{T_1}}{2(\sigma^2_{T_1}/(N^2_\alpha N^2_\beta)}) \tag{16}$$

Remembering that the probability for the CorrPower Γ will need to take the maximum value of gamma among 3 different integration windows

$$P(\Gamma) = P(\Gamma = max(r_{T_1}, r_{T_2}, r_{T_3})) \tag{17}$$

We will need to calculate a joint probability density function for the Γ among the 3 different integration windows. since r_{T_1}, r_{T_2}, and r_{T_3} are all Gaussian random variables their joint probability is Gaussian too. Unfortunately r_{T_1}, r_{T_2}, and r_{T_3} are correlated. In order to evaluate the correlation matrix and therefore the joint probability density function we assume that the data that maximizes the shortest coincident window is included in the data that maximizes the next in duration coincident window, which in turn will be included in the data containing the longest coincident window. With these assumptions at hand the joint PDF becomes:

$$P(r_{T_1}, r_{T_2}, r_{T_3}) = \frac{1}{\sqrt{2\pi det\mathbf{C}}} exp(-\mathbf{r}\mathbf{C}^{-1}\mathbf{r}) \tag{18}$$

with

$$\mathbf{r} = (r_{T_1}, r_{T_2}, r_{T_3}) \tag{19}$$

and

$$\mathbf{C} = \begin{pmatrix} \sigma^2_{T_1} & \sigma^2_{T_1} & \sigma^2_{T_1} \\ \sigma^2_{T_1} & \sigma^2_{T_1} + \Delta^2_1 & \sigma^2_{T_1} + \Delta^2_1 \\ \sigma^2_{T_1} & \sigma^2_{T_1} + \Delta^2_1 & \sigma^2_{T_1} + \Delta^2_2 \end{pmatrix}. \tag{20}$$

and

$$< r_{T_1} r_{T_2} >= \sigma^2_{T_1} \tag{21}$$

$$< r_{T_2} r_{T_3} >= \sigma^2_{T_1} + \Delta^2_1 \tag{22}$$

$$< r_{T_1} r_{T_3} >= \sigma^2_{T_1} \tag{23}$$

$$< r_{T_2} r_{T_2} >= \sigma^2_{T_1} + \Delta^2_1 \tag{24}$$

$$< r_{T_3} r_{T_3} >= \sigma^2_{T_1} + \Delta^2_2 \tag{25}$$

$$\Delta^2_1 =< r^2_{T_\alpha} >, \Delta^2_2 =< r^2_{T_\beta} > \tag{26}$$

The last two equations describe the same summations involved in equation 21 but over the time included in T_2 which is not included in T_1: where T_α and the time in T_3 which is not included in T_1, T_β. They assume that the data in T_1 and T_α and T_β. are uncorrelated because they are sufficiently temporally separated.

$$P = (max(r_T) = R) = \frac{1}{3}[P(r_{T_1} = R, r_{T_2} < R, r_{T_3} < R) + P(r_{T_1} < R, r_{T_2} = R, r_{T_3} < R) + P(r_{T_1} < R, r_{T_2} < R, r_{T_3} = R)] \tag{27}$$

The equation above requires integrating 19 for 2 of the 3 random variables.
To maximise our statistic versus τ.....τ will be fixed anyway by the presence of the injection.

$$\begin{aligned} \hat{r}_T &= \sum_{i=1}^{N} (x_\alpha(t_i) + h_\alpha(t_i))(x_\beta(t_i + \tau) + h_\beta(t_i + \tau))\Delta t \\ &= \sum_{i=1}^{N} (x_\alpha(t_i)x_\beta(t_i + \tau) + x_\alpha(t_i)h_\beta(t_i + \tau) + h_\alpha(t_i)x_\beta(t_i + \tau) + h_\alpha(t_i)h_\beta(t_i + \tau))\Delta t \end{aligned}$$

$$< \hat{r}_T >= \sum_{i=1}^{N} < h_\alpha(t_i) >< h_\beta(t_i + \tau) > \Delta t \tag{28}$$

$$
\begin{aligned}
< (\hat{r}_T - < \hat{r}_T >)^2 > &= \sum_{i=1}^{N}\sum_{j=1}^{M}(x_\alpha(t_i)x_\beta(t_i+\tau) + x_\alpha(t_i)h_\beta(t_i+\tau) + h_\alpha(t_i)x_\beta(t_i+\tau) \\
&\quad + h_\alpha(t_i)h_\beta(t_i+\tau))(x_\alpha(t_j)x_\beta(t_j+\tau) + x_\alpha(t_j)h_\beta(t_j+\tau) + h_\alpha(t_j)x_\beta(t_j+\tau) + h_\alpha(t_j)h_\beta(t_j+\tau)) \\
&= \sum_{i,j=1}^{N} R_\alpha(t_i-t_j)R_\beta(t_i-t_j) + \sum_{i,j=1}^{N} R_\alpha(t_i-t_j)h_\beta(t_i-\tau)h_\beta(t_j+\tau) + \sum_{i,j=1}^{N} R_\beta(t_i-t_j)h_\alpha(t_i)h_\beta(t_j) \\
&= \sum_{i,j=1}^{N} R_\alpha(t_i-t_j)R_\beta(t_i-t_j) + \sum_{i,j=1}^{N} R_\alpha(t_i-t_j)h_\beta(t_i)h(t_j) + \sum_{i,j=1}^{N} R_\beta(t_i-t_j)h_\alpha(t_i)h_\alpha(t_j)
\end{aligned}
$$

The average value of the r statistic for a given window is given by Equation 11 where the numberator is replaced by Equation 32. Since the signal is pre-whitened before going to the r statistic, the current derivation is correct provided both signal and noise are whitened. As discussed previously, we calculate Γ for windows of 10, 25 and 50 ms, then take the largest of the three. For interferometers α and β, $\Gamma_{\alpha\beta}$ for a given time window is calculated by finding the maximum of

$$\Gamma_{\alpha\beta} = -log_{10}(erfc(abs(r).\sqrt{N_{eff}/2})) \tag{29}$$

over all possible time shifts of one interferometer with respect to the other. For signal injections, we take this to be the correlation of the injection with itself with no time lag. Equation 29 is basically just the logarithm of the correlation's statistical significance and is defined by lines 352 – 354 of *CCpixel.m* in the CorrPower source code. It matches the description given in P050012-00.pdf. $N_{eff}/2$ is just the number of samples in the integration window (plus 1/2 by definition):

$$
\begin{aligned}
0.5 + \frac{10ms}{1000ms}.16384 &= 164.5 \\
0.5 + \frac{25ms}{1000ms}.16384 &= 410.5 \\
0.5 + \frac{50ms}{1000ms}.16384 &= 820.5
\end{aligned}
$$

r is the correlation function given in equation (2). As discussed above, the assumption of stationarity allows us to take the correlation of noise between the two interferometers to be negligible, so $x_\alpha x_\beta$ is really just the correlation between the two signals, $s_\alpha s_\beta$. Likewise, we assume that correlation between signal and noise is approximately zero on average so that the norm is just the power in the signal plus the power in the noise. Plugging this into equation 11 (I have used "s" here for signal while "S" has been defined above as the noise spectral densities):

$$r = \frac{\int_{-T/2}^{T/2} s_\alpha s_\beta dt}{\sqrt{\int_{-T/2}^{T/2} n_\alpha^2(t)dt + \int_{-T/2}^{T/2} s_\alpha^2(t)dt}\sqrt{\int_{-T/2}^{T/2} n_\beta^2(t)dt + \int_{-T/2}^{T/2} s_\beta^2(t)dt}} \tag{30}$$

The data are whitened, which changes the calculation a bit. Going from time to frequency domain, the noise calculation becomes straightforward because the noise power spectral density is normalized to $n^2(f) = 1$ at all frequencies.

$$n_{tot}^2 = \Delta t \int_{f_{low}=1000}^{f_{high}=6500} n^2(f)df = 5500\Delta t \tag{31}$$

So, $n_{tot}^2(10ms) = 55$, $n_{tot}^2(25ms) = 138$ and $n_{tot}^2(50ms) = 275$. Ignoring antenna pattern for the moment (since we will generally take the antenna pattern to be the same in each interferometer for the purpose of this estimate), without whitening, $\int_{-T/2}^{T/2} s_\alpha^2(t)dt$ would just be the same as h_{rss}^2 (where h_{rss} is the variable we want to plot on the x-axis of our comparison plots). However, we need to perform whitening on the signal as well as the noise, so we divide our h_{rss} value by the square root of the noise power spectral density. The noise spectral density is determined experimentally (using ASCII files containing official strain curves from `http://www.ligo.caltech.edu/~jzweizig/distribution/LSC_Data/`). The effect on signal power from the noise floor at each frequency must be weighted by that frequency's total contribution to the signal energy. The frequency content of a Q=9 sine Gaussian is:

$$h(f) = \frac{1}{\sigma\sqrt{2\pi}} exp(\frac{(f-f_c)^2}{2\sigma^2}), \sigma = f_c/Q = f_c/9 \tag{32}$$

	2000 Hz Early S5	2000 Hz Later S5	5000 Hz Early S5	5000 Hz Later S5
H1	2.62×10^{-22}	2.27×10^{-22}	6.90×10^{-22}	6.22×10^{-22}
H2	5.06×10^{-22}	3.59×10^{-22}	2.20×10^{-22}	1.37×10^{-21}
L1	2.90×10^{-22}	2.61×10^{-22}	7.29×10^{-22}	7.04×10^{-22}
design 4k		2.49×10^{-22}		6.22×10^{-22}

So we weight our relative noise contribution at each frequency and get our noise floor according to the formula:

$$m_{f,\alpha} = \sqrt{\frac{\int_{f_{low}}^{f_{high}} n^2(f)[\frac{1}{\sigma\sqrt{2\pi}} exp(\frac{(f-f_c)^2}{2\sigma^2}]^2 df}{\int_{f_{low}}^{f_{high}} [\frac{1}{\sigma\sqrt{2\pi}} exp(\frac{(f-f_c)^2}{2\sigma^2}]^2 df}} \tag{33}$$

In practice, this integral is carried out as a summation over discrete frequency values in *injectionweightednoisefloor.c*, which takes two arguments: noise spectrum file and central frequency. Our denominators to normalize our h_{rss} values for whitened data are given below for 3 frequencies and measured noise spectra from two points in the run:

So, for a given time window, our Γ as a function of h_{rss} (averaging over the Γs between each IFO pair) is:

$$\Gamma = \frac{1}{3} \sum^{ifopairs} -log_{10}[erfc(\frac{h_{rss}^2 \sqrt{N_{eff}/2}/m_{f,\alpha} m_{f,\beta}}{\sqrt{(n_{tot}^2 + h_{rss}^2)/m_{f,\alpha}^2} \sqrt{(n_{tot}^2 + h_{rss}^2)/m_{f,\beta}^2}})] \tag{34}$$

for any value of $h_{\rm rss}$, with the other values as already defined.

The two figures below plot the Γ values versus the injected $h_{\rm rss}$ averaged over the two detector sites for sine-Gaussians at two central frequencies (2 kHz and 5 kHz). The line plots the integral estimates of the expected Γ values as a function of h_{rss} using noise curves taken from two points during the S5 run. The *Late 1st year* noise curves were taken when the detectors were running better than during *Early 1st year*. The software injections, represented by the red scatter, follow a similar trend to the curves from the analystic estimate.

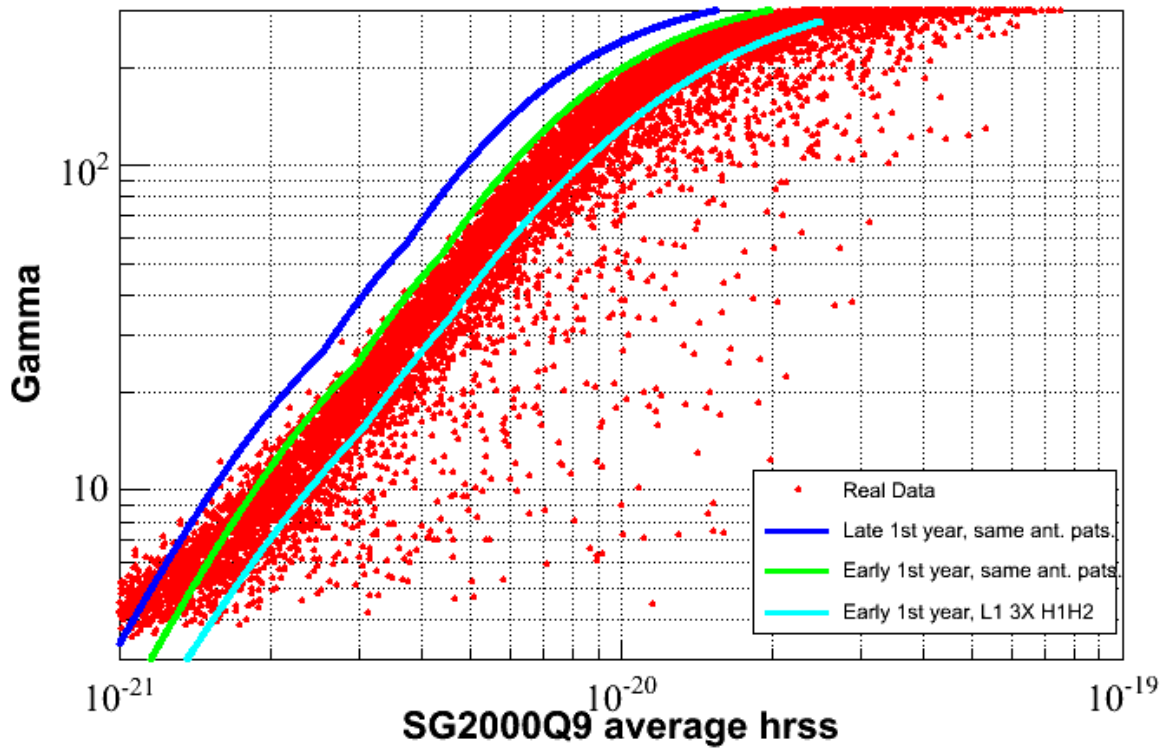

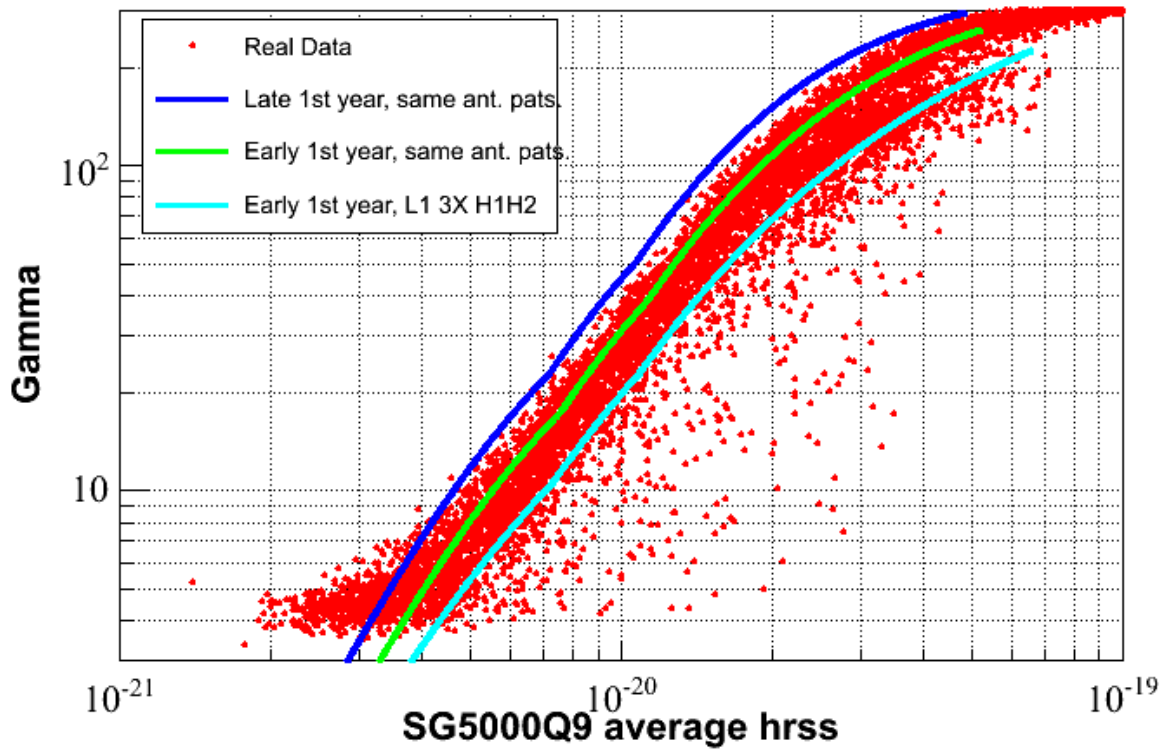

For the 2 kHz sine-Gaussians, the sensitivity estimate was also recalculated using Shourov's median noise curves. The resulting curve was nearly identical to the "Late 1st year" curve in the figure above.

The range of the red scatter can be explained by the varying antenna pattern between the two detector sites. For some injections, there is a large difference in antenna patterns between the two sites. The Γ value is significantly reduced for these injections since the signal is dominated by noise in at least one of the detectors. Injected signals with bad Hanford antenna patterns produce the smallest Γ values. A follow-up of about 10 injections found in the bottom right hand corner of the plots found that all these injections had antenna patterns that produced a small signal at the Hanford detectors.

To demonstrate the antenna pattern effect on the analytic estimate, the calculation is performed for a situation where the L1 antenna pattern is 3 times that of H1H2. The calculated Γ values are now reduced for the corresponding $h_{\rm rss}$ and is represented by the light blue curve.

[1] Paper draft https://www.lsc-group.phys.uwm.edu/cgi-bin/pcvs/viewcvs.cgi/bursts/papers/HFSdraft/HFSpaper.pdf?cvsroot=lscdocs
[2] Review summary table https://www.lsc-group.phys.uwm.edu/bursts/review/projects/s5-qpipe-highf/summaryTable.html
[3] Post-processing and plot script checks http://www.astro.gla.ac.uk/~matthew/blog/?page_id=226
[4] Checks on data quality flag application https://www.lsc-group.phys.uwm.edu/bursts/review/projects/s5-qpipe-highf/misc/dq_flag_review.html
[5] Report on the debugging of the R0:H1H2 issue and its effects on the results http://emvogil-3.mit.edu/~bhughey/high_freq_search/CorrPowerR0bugreport.html
[6] H1H2 analysis webpage http://ldas-jobs.ligo.caltech.edu/~jackie/home.html
[7] Checks on Baiotti and Rezzolla waveform data conditioning https://ldas-jobs.ligo.caltech.edu/~jkanner/q-hfs/astroWaves.html
[8] Sensitivity estimate http://emvogil-3.mit.edu/~bhughey/high_freq_search/CorrPowerSensitivity/